

## Review Article

# A Status Review on $\text{Cu}_2\text{ZnSn}(\text{S}, \text{Se})_4$ -Based Thin-Film Solar Cells

**Sudipto Saha** 

*Electrical and Computer Engineering, North Dakota State University, Fargo ND 58102, USA*

Correspondence should be addressed to Sudipto Saha; [sudipto.saha@ndsu.edu](mailto:sudipto.saha@ndsu.edu)

Received 28 March 2020; Accepted 15 August 2020; Published 1 September 2020

Academic Editor: Ahmad Umar

Copyright © 2020 Sudipto Saha. This is an open access article distributed under the Creative Commons Attribution License, which permits unrestricted use, distribution, and reproduction in any medium, provided the original work is properly cited.

Photovoltaics has become a significant branch of next-generation sustainable energy production. Kesterite  $\text{Cu}_2\text{ZnSn}(\text{S}, \text{Se})_4$  (copper-zinc-tin-(sulfur, selenium) or CZTS(Se)) is considered one of the most promising, earth-abundant, and nontoxic candidates for solar energy generation over the last decade. However, shallow phase stability of the quaternary phase and the presence of various secondary phases and defects are the main hindrances in achieving the target device performance. This paper summarizes various approaches to synthesize the CZTS absorber layer and the CdS *n*-type material layer. Besides, different CZTS solar cell device structures, as well as a comprehensive review of secondary phases and defects, have been illustrated and discussed. At last, this review is intended to highlight the current challenges and prospects of CZTS solar cells.

## 1. Introduction

With the exponential burgeon of the population, the consumption of traditional energy has escalated at an eminent rate. This enormous demand for power is mostly satisfied by fossil fuels. However, these fossil fuels are limited resources. Moreover, the combustion of them produces exhausting gases that are detrimental to the global environment. As this inflation in the use of conventional energy is heading towards a worldwide environmental crisis, solar cell technology has drawn the attention of the researchers. Approximately 80% of the current photovoltaic market is based on c-Si and pc-Si wafers [1, 2]. However, because of its indirect bandgap and imperfect crystal structure, Si-based solar cell technology is leaving the market for direct bandgap thin-film technology. At present, most common thin-film materials are copper indium gallium diselenide (CIGS), copper indium diselenide (CIS), cadmium telluride (CdTe), gallium arsenide, and the copper-zinc-tin-sulfur (CZTS). Energy harvesting through thin-film photovoltaics is environmentally clean and efficient because of its decreased material cost and flexibility in the deposition on various substrates. However, gallium arsenide and cadmium telluride contain toxic cadmium and arsenic.

However, the record efficiency of CIGS produced in the laboratory is 22.6% [3]. Application of heavier alkali elements rubidium and cesium in the alkali postdeposition treatment (PDT) has enabled reaching this much efficiency. However, the presence of rare indium is the main hindrance to the future widespread development of CIGS solar cells.

CZTS is a promising replacement for conventional materials in thin-film solar cell technology, having efficiency over 10% [4, 5]. Though record conversion efficiency of 12.6% was recorded for CZTSe [6], due to the toxicity of Se, pure sulfide CZTS is preferable. CZTS cells have a high absorption coefficient (up to  $10^5 \text{ cm}^{-1}$ ) [7], which is very competitive to CIGS thin-film solar cells. This momentous optical absorption efficiency, along with appropriate direct bandgap (1.0-1.5 eV), helps CZTS cells to convert solar energy into electricity with significantly high efficiency. The composing elements of CZTS cells—copper, zinc, and tin—are abundant in nature and cost-effective. The chemical molecular structure makes CZTS cells more stable than CIGS solar cells [8]. So, CZTS cells require less restoration cost, which makes it more economically competitive in the long run. Cation alloying offers independent adjustment of the absolute position of the valence band and conduction band [9]. Moreover, low toxicity, tunable

bandgap, comparatively better performance in indirect light and high temperature, and more utility in flexible thin-film operations have made CZTS thin-film solar cells one of the most promising candidates in renewable energy harvesting.

Though until now, CZTS thin-film solar cells have just surpassed 11% border [10]; senior theoretical estimates of about 27.5% [8] make this more auspicious. One of the significant drawbacks that limit the power conversion efficiency of CZTS solar cells is its phase homogeneity and the presence of secondary phases. CZTS phase is stable for a narrow region, and it shares boundaries with other secondary phases. The indirect control over the composition and volatile nature of Zn and Sn make the condition more resilient. According to the experimental results, the confined stable chemical potential range results in detrimental effects [11–13]. Also, relatively small grain size causes more defects and grain boundaries, which leads to a higher recombination rate and lower efficiency. Again, the chemical bonding between anion p orbitals and Cu d orbitals engenders an upward shift of the Valence Band Maximum, VBM, and degradation of the ionization potential of s-p bonding semiconductor from the standard value [9]. Other common issues are multivalent Sn (i.e., II and IV oxidation states) and nonohmic back contact [14]. All these problems constitute a degraded CZTS solar cell performance than expected.

This paper aims to discuss different fabrication processes of CZTS absorber materials and CdS *n*-type materials. Moreover, the paper not only provides insights for different device structures but also makes aware of the secondary phases, defects, optical, and electrical properties of CZTS thin-film solar cells.

## 2. About CZTS

The quaternary CZTS semiconductor material has two different crystalline forms—stannite and kesterite. Both of them are a  $1 \times 1 \times 2$  tetragonal expansion of zinc-blende with different space groups, I-4 and I-42m, respectively (Figure S1) [15]. The difference between the lattice parameters and total energy values are infinitesimal. Hence, there is a possibility of the coexistence of both phases existing together, depending on the preparation methods.

CZTS outsmarts many already present commercialized photovoltaic devices such as CIGS and CdTe with its auspicious optoelectronic properties. Because of having some favorable characteristics for photovoltaic devices, CZTS has already been utilized in different photovoltaic device structures. The composing elements of CZTS thin film—copper, zinc, tin, and sulfur—are more feasible and readily available in the market [16]. Besides, the optimum bandgap required for semiconducting photovoltaics (~1.5 eV) is very close to the bandgap of CZTS (1.4–1.5 eV). Moreover, the high absorption coefficient permits CZTS to be employed as an absorber layer in multiple-layer-based photovoltaic structures. On top of that, low toxicity, tunable bandgap, comparatively better performance in indirect light and high temperature, and more utility in flexible thin-film operations have made CZTS thin-film solar cells one of the most promising candidates to harvest renewable energy.

## 3. Synthesis of CZTS(Se)

Various synthesis methods have been adopted in the last two decades for the deposition of CZTS(Se). The synthesis can be of either one step or two steps. In most of the two-step fabrication techniques, the CZT metal precursor is prepared first, then sulfurized/selenized and annealed to develop CZTS(Se). On the contrary, in one-step fabrication techniques, CZTS(Se) is directly produced, followed by heat treatment. The efficiency of the device depends on factors such as deposition rate, layer thickness, and synthesis method adopted.

**3.1. Sputtering.** Sputtering is a prevalent method of fabrication that offers uniformity and reproducibility of deposited layer on a large scale [17–20]. This method is suitable for large scale solar cell production with control over interface engineering, tuning of crystallinity, and the composition of the films [21, 22]. Sputtering is usually performed in three different mechanism—sequential sputter deposition of precursor films, deposition of precursor film by cosputtering, and single-target sputtering.

**3.1.1. Sequential Sputter Deposition.** Sequential deposition of precursors followed by sulfurization/selenization is an extensively practicing technique for the synthesis of CZTS(Se) thin films [23, 24]. Optimization of the composition plays a vital role in characterizing the cell performance. Most high-efficiency CZTS(Se) solar cells have a Cu-poor and Zn-rich composition of the absorber layer. The thickness of the stacked precursors controls the composition of deposited CZTS(Se). Sulfurization/selenization is another crucial step for converting the stacked precursors' layer into CZTS(Se). Sulfurization/selenization time, temperature, pressure, weight, and source of sulfur/selenium are pivotal for CZTS(Se) film properties [25]. However, the high-temperature treatment causes the loss of Sn [26], which eventually results in the formation of  $\text{Cu}_{2-x}\text{S}$  secondary phase at the film surface [27] and degradation of CZTS(Se) stoichiometry, and cracks and holes in the grain boundaries. Sugimoto et al. reported that lower Cu/Sn ration results in longer photoluminescence lifetime and wider bandgap, thus improving  $V_{oc}$ . Thus, the prevention of Sn loss seems to be crucial to suppress secondary phase formation and fabricate CZTS thin films of high quality [28].

Several approaches to suppress the loss of volatile species for CZTS films prepared by sulfurization of stacked precursors were reported to date. Wei et al. annealed the stacked precursor before sulfurization and enhanced the crystallinity of CZTS absorber, reducing evaporation. A method to reduce the evaporation of volatile compounds by performing rapid thermal sulfurization of stacked precursor layers for 5 min was reported by Pawar et al. [29]. Gang et al. could reduce Sn-loss by increasing sulfur partial pressure [26].

**3.1.2. Cosputtering.** The cosputtering technique can also be used as an effective way to produce uniform CZTS(Se) films [30–33]. Feng et al. fabricated a CZTS photovoltaic device using a cosputtering technique followed by two-step treatment and reported better energy conversion efficiency of 5.85% with higher hole concentration and lower defect density than conventional CZTS device with one-step annealing [34]. Scragg et al. prepared the CZTS device from

reactive cosputtering of Cu/Sn alloy and Zn targets followed by sulfurization in the  $H_2S$  atmosphere and reported efficiency of 4.6% [35]. A substrate temperature of  $120^\circ C$  was maintained during the deposition. It has been reported that the grain size of the annealed film was about  $1 \mu m$ . Cormier et al. fabricated CZTS films in a one-step process by cosputtering of Cu/Sn alloy and Zn targets in  $Ar/H_2S$  atmosphere using heated substrate and reported that temperatures higher than  $300^\circ C$  is essential for crystallized CZTS thin films [36].

**3.1.3. Single Target Sputtering.** Single target sputtering of CZTS(Se) is mostly favorable for large-scale manufacturing of CZTS(Se)-based photovoltaic devices. This scheme is simple and cheap and ensures uniform element distribution within deposited films. This single-target approach also requires less sulfurization/selenization temperature and time compared to stacked-layer sputtering. Nakamura et al. compared cosputtered CZTS from Cu/ZnS/SnS targets with single target CZTS sputtering and reported similar chemical, optical, and crystalline properties. However, CZTS prepared from single target sputtering were void-free, whereas cosputtered CZTS films contained voids [37]. Jheng et al. varied the substrate temperature while depositing CZTS thin film in a single target sputtering method and reported the substrate temperature of  $150^\circ C$  as optimal concerning carrier concentration, carrier mobility, and resistivity [38]. They investigated that the increase of substrate temperature caused a significant reduction of sulfur content, an increment of the copper content in the as-grown films, and a decrease in strain and dislocation density in the deposited films.

**3.2. Hot Injection.** The hot injection is a scalable and straightforward method of synthesizing CZTSSe nanocrystals. It is a rapid promising technique and can be used for a large scale synthesis. CZTSSe nanocrystal has been developed using different approaches such as single-step colloidal CZTSSe synthesis, binary and ternary colloidal nanocrystal synthesis, and synthesis of CZTSSe nanocrystals using alloying with Ge or defect passivation of Na. In general, Cu, Zn, and Sn-based precursors are chosen and dissolved in complexes with long-chain coordinating solvents. Then, sulfur or a selenium source is injected at a controlled temperature for nucleation and controlled growth. The metal chloride, acetate, and acetylacetonate precursor compounds are previously reported as precursor sources. Oleylamine (OLA), oleic acid (OA), trioctylphosphine oxide (TOPO), and octadecene (ODE) have been reported previously as coordinating solvents with high boiling points. Thiourea, dodecanethiol (1-DDT), and tertdodecyl mercaptan (t-DDT) or the elemental sulfur are used as sulfur sources, which also controls the crystal growth as well. Though the CZTSSe-based solar cells are still in the developing stage, they offer promising room for future improvement.

Kim et al. first developed pure CZTS nanocrystal-based solar cell devices with an efficiency of 3.6% [39]. The maximum quantum efficiency of 50% was obtained at a photon wavelength of 550 nm. The holes and cracks in the nanocrystals caused low shunt resistance and high series resistance. This results in low energy conversion efficiency. CZTSSe nanocrystal-based devices showed better performance

compared to pure CZTS nanocrystal-based solar cells. Guo et al. first deposited the CZTSSe nanocrystal-based absorber layer by the selenization of CZTS nanocrystals thin films in 2009 [40]. The efficiency was 0.8% for  $500^\circ C$ . In the next year, they tuned the composition to Cu-poor and Zn-rich and improved the efficiency to 7.2% [41]. Recently, the same group has achieved 9.0% efficient CZTSSe nanocrystals-based solar cells, which is the best-reported performance for the hot injection-based method. Cao et al. fabricated CZTSSe thin films with the desired composition from combining an appropriate mixture of synthesized binary and ternary nanocrystals followed by annealing in the presence of Se that allows facile control over the film composition [42]. They obtained a promising efficiency of 8.5% which is one of the highest efficiencies for CZTSSe photovoltaics.

**3.3. Pulsed Laser Deposition (PLD).** Pulsed laser deposition is a versatile and straightforward method of depositing a wide range of materials that offer a high deposition rate, the easy transformation of materials from target to substrate, and reactive deposition. The overall deposition process of CZTSSe thin films can be divided into three consecutive segments—formation of CZTS target, irradiation of laser beam on the CZTSSe target, and annealing of as-deposited CZTS thin films along with selenization. Generally, a CZTS pellet, formed from the mechanochemical or solid-state reaction, is used as a target. Binary chalcogenide powders such as  $Cu_2S$ , ZnS, and  $SnS_2$  are used to form the CZTS phase. After that, a high-power pulsed laser beam is focused inside an ultrahigh vacuum chamber to strike the CZTS target. CZTS material is evaporated from the target in a plasma plume, which is deposited on a substrate as a thin film. The fabricated film properties vary enormously with the variation of any of the parameters such as pulse repetition rate, pulse energy, target material, target-to-substrate distance, and substrate temperature. The as-deposited CZTS thin film is amorphous and is annealed at a temperature higher than transition temperature to transform it into polycrystalline nature. The annealing temperature and duration play a crucial role in determining the structural, optical, electrical, and morphological characterization of thin films. Selenization of as-deposited CZTS film is performed along with annealing in the case of CZTSSe thin-film fabrication.

Historically, Sekiguchi et al. applied the PLD for the first time to deposit CZTS thin films on GaP substrates at varying substrate temperature [43]. The CZTS thin films deposited at substrate temperatures of  $350^\circ C$  and  $400^\circ C$  were nearly stoichiometric. Moriya et al. reported, for the first time, the solar cell application of CZTS grown in the PLD approach. They annealed the as-deposited CZTS in  $N_2$  and  $N_2+H_2S$  atmosphere [44, 45]. Though the CZTS composition was nearly stoichiometric in  $N_2+H_2S$  atmosphere, the device annealed in  $N_2$  atmosphere gave better conversion efficiency.

According to Moriya et al., the optimization of precursor composition was necessary. Sun et al. deposited CZTS both in sputtering and pulse laser deposition approach and reported better stoichiometry for PLD compared to the sputtering approach [46]. Sputtered CZTS thin films show more structural defects compared to pulse laser deposited CZTS.

This report underlines the importance of the PLD technique in CZTS thin-film formation.

**3.4. Sol-Gel.** This sol-gel method of fabrication has some advantages over other nonvacuum approaches. Firstly, this technique is straightforward and cost-effective for synthesizing the powder samples with needed stoichiometry. Moreover, in this method, the cation can be substituted easily to improve solar cell performance. This method makes the hydrolyzable metal compound to react with water in certain solvents to form as Sol by hydrolysis and polycondensation. A chelating agent is also added to the solution to increase the stability of the ion-complex. The sol is then either spin-coated or stirred to form a liquid film on the substrate [47, 48]. Then, it is dried in air to remove residual organic materials. The deposition process is repeated several times until the required thickness is achieved. The resulting CZTS thin film is soaked in DI water to remove the oxidation phase with high resistance. Selenization is required during annealing to get CZTSSe thin films.

Miyamoto et al. reported the first photoluminescence of a CZTS film on films prepared by a sol-gel sulfurization method [49]. Tanaka et al. fabricated a CZTS absorber layer for a solar cell in which the sol-gel method was employed in 2007 [50]. They used cupric acetate, zinc acetate, and tin chloride as precursor sources to prepare sol gelatin in the dimethyl alcohol solvent and the ethanolamine stabilizer mixer. The spin-coated film was annealed at 500°C in N<sub>2</sub> atmosphere. In 2011, the power conversion efficiency of 2.03% was achieved by the same group of researchers with the aid of optimizing film components [51].

**3.5. Spray Pyrolysis.** Spray pyrolysis is a nonvacuum approach of preparing CZTSSe thin films because of its cost-effectiveness and easy deposition of films in the large area. The composition of the film can be controlled efficiently and smoothly. In the spray pyrolysis technique, the substrate is heated, and one or more metalloorganic compounds or metal salts dissolved in aqueous or organic solvents are sprayed onto the substrate surface. Solute concentrations in the spray solution are used to control the chemical composition of the films. The temperature gradient leads to the pyrolysis of the spray coating and deposits a thin film on the substrate. The substrate temperature plays a crucial role in determining the thin film performance. When the substrate temperature is very high, the film adsorption on the substrate becomes difficult.

On the contrary, too low substrate temperature deteriorates the crystallization of the film. Spray pyrolysis process of CZTS thin-film prefers substrate temperature inside the range of 500-650°C [1]. Annealing and selenization of the deposited CZTS films are performed in a furnace at a temperature of 500-600°C for about an hour to prepare CZTSSe thin film. Kamoun et al. prepared a solution of CuCl<sub>2</sub>, ZnCl<sub>2</sub>, and SnCl<sub>2</sub> and vulcanized them in SC(NH<sub>2</sub>)<sub>2</sub> solution using the spray pyrolysis technique. The substrate temperature was 340°C, and the deposited film was annealed for 2 hrs at 550°C. Eventually, the CZTS-based thin films with a bandgap of 1.5 eV were fabricated. Moreno et al. used dimethyl sulfoxide (DMSO) as solvent [52]. Thiourea is usually the source of sulfur and Cu-thiourea complex in the precursor solution is

not expected, and to prevent it, the pH of the precursor solution needed to keep constant. The addition of a few drops of concentrated nitric acid in the solution does the job [53].

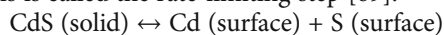
**3.6. Electrochemical Deposition.** CZTSSe thin films are synthesized in this nonvacuum method as large-area film preparation requires cheaper precursors and simple setup in this method. Moreover, the electrochemical deposition technique is preferred because of the high utilization of raw materials and close control of composition. CZTS-based thin-film photovoltaics are usually fabricated by using soda-lime glass (SLG) and molybdenum (Mo)-coated substrates. Before deposition, the substrate foil is cleaned in acetone, isopropanol, and ethanol sequentially. CZTSSe films are prepared either as stacked metallic layers of Cu, Zn, and Sn or codeposition of Cu-Zn-Sn. The film is electrochemically deposited using a conventional 3-electrode cell with a platinum counter electrode and a reference electrode. The as-deposited film is annealed in a sulfur/selenium atmosphere to form CZTSSe films at about 500°C.

Scragg et al. reported the first-ever electrodeposition method of preparing CZTS-based solar cells [54]. He deposited Cu-Sn-Zn sequentially from metal chloride solutions mixed with NaOH and sorbitol. Recently, they have prepared metallic layers in the stacking order of Cu/Sn/Cu/Zn followed by sulfurization at 575°C in the N<sub>2</sub> atmosphere and reported overall power conversion efficiency of 3.2% [55]. Ennaoui et al. fabricated CZTS solar cells through the one-step codeposition technique of ternary alloys of Cu-Zn-Sn layers were first prepared by electrochemical deposition followed by annealing in Ar+H<sub>2</sub>S atmosphere [56]. They reported the best cell performance of 3.4% for Cu-poor samples. A light treatment after deposition resulted in an enhanced photovoltaic performance of 3.59% [57]. Araki et al. fabricated Zn-rich CZTS films in the electrodeposition method using an electrolyte solution metal salts and trisodium citrate dihydrate followed by sulfurization at 600°C for 2 hrs in the carrier gas containing sulfur powder in 2009 [58]. They reported the energy conversion efficiency of 3.16%. In 2011, Ahmed et al. achieved an efficiency of 7.3% from stacked metal electrodeposition followed by sulfurization, which is one of the best solar cell performances in this method [59].

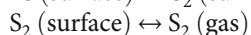
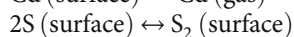
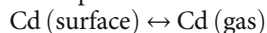
**3.7. Synthesis of the CdS Layer.** Cadmium sulfide (CdS) is a wide bandgap semiconductor material which is extensively employed for the fabrication of superstrate type solar cell structures. Its low resistivity and high transmissivity [51, 60, 61] have made it a good candidate for efficient window material. CdS can be fabricated in various techniques including electrodeposition [62], spray pyrolysis [63], sputtering [64], thermal evaporation [65], sintered and screen printing [66, 67], and chemical bath deposition [68]. Among all the processes, CBD is the prevalent process to make very thin CdS thin film for solar cells, and RF sputtering is used very often to get CdS thin films with a very smooth surface.

**3.8. Thermal Evaporation.** Thermal evaporation is one of the most common techniques for the deposition of CdS. In this

method of deposition, a solid material is placed in a quartz or carbon ampoule and heated to the point where the solid material starts to evaporate and later condenses onto a cooler substrate to form a film. The ampoule is chosen so that it prevents the chemical attack of the heated metal source. The process of thermal evaporation has four main steps. At first, bulk CdS dissociates to cadmium and sulfur on the surface. This is called the rate-limiting step [69].



Cd atoms are barely bounded on the surface and evaporate directly. But the single S atoms associate and form  $\text{S}_2$  before evaporation.



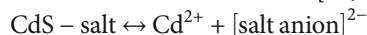
The evaporation rate depends largely on the crystal evaporation face. CdS films grow in parallel to the  $c$ -axis at a faster evaporation rate. So the  $c$ -axis is expected to be normal to the substrate for the fastest evaporation. Besides the orientation, the substrate temperature also affects the stoichiometry and electrical and optical properties of thermally evaporated CdS [70–72]. Because of the difference in vapor pressure between Cd and S elements, it is difficult to maintain the stoichiometry of thermally evaporated CdS. Coevaporation or flash evaporation is suitable in this regard [73, 74].

**3.9. Sputtering.** Sputtering is considered preferable to thermal evaporation for the deposition of CdS, mostly because of higher material utilization during the deposition on the substrate. This method provides highly pure thin films and prevents the accumulation of excess electric charges on the surface of the target. As the optical and electrical properties mostly depend on the uniformity of the orientation of the  $c$ -axis of CdS, sputtering provides much more uniformity than thermal evaporation for large scale deposition. The electrical and optical properties of sputtered films depend on the sputtering parameters such as sputtering time and substrate temperature. By controlling the sputtering time, the thickness of the CdS layer can be adjusted. Annealing temperature and duration play an important role in film characterization.

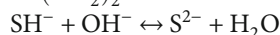
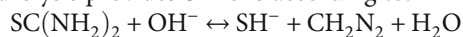
**3.10. Spray Pyrolysis.** Spraying of the cadmium-sulfide layer is a nonvacuum technique and would be ideal for industrial applications. This technique offers stoichiometry and high deposition rates. The process involves the spraying of a solution of a cadmium salt and a sulpho-organic compound on to a heated substrate [75]. The sprayed solution is diluted either in water or alcohol or both. The subsequent reaction on the hot substrate produces a CdS film and volatile products. The quality of the films produced by this technique depends upon some parameters such as spray rate, substrate temperature, droplet size, cooling rate, carrier gas, and ambient atmosphere [76]. The substrate temperature should be between 350 and 500°C [77, 78]. For temperature less than 350°C, the crystal lattice size of deposited CdS is usually small with a rough surface. For temperatures above 350°C, CdS is deposited as a smoother layer with large crystallites and good  $c$ -axis alignment normal to the substrate.

**3.11. Screen Printing Followed by Sintering.** Screen printing is an inexpensive and convenient technique for large-area preparation of the films [79, 80]. In particular, screen printing is low cost and relatively simple technique for achieving good optical properties and high mobilities. This technique is suitable for coating surfaces with different morphology and geometry. This technique uses a woven mesh to support an ink-blocking stencil and transfer ink onto a substrate. Arita et al. have grown CdS thin film by this technique in 1991 using CdS paste deposited on a glass substrate [81]. These layers are formed by mixing CdS powder with  $\text{CdCl}_2$  in a slurry and then firing. The  $\text{CdCl}_2$  in the slurry acts as a flux for the crystallization of CdS. Then, the material is ball-milled in a slurry adding a binding agent such as ethylene glycol. The slurry can be applied to a substrate by spraying or screen printing and is then annealed at 500–600°C [82].

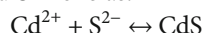
**3.12. Chemical Bath Deposition (CBD).** Chemical bath deposition is a widely used simple and large area deposition technique that requires low temperature. In CBD method, CdS thin films are prepared by decomposing thiourea ( $\text{SC}(\text{NH}_2)_2$ ) in an alkaline solution containing Cd-salt and suitable complexing agent ammonia and ammonium chloride. In this method, Cd-salt serves as the cadmium source, and thiourea is the sulfur source. The solution is homogenized by stirring at low temperature (e.g., 80° Celsius) and keeping the pH constant at about 10. CdS thin films are deposited by the reaction of  $\text{Cd}^{2+}$  complex supplied by Cd-salt and  $\text{S}^{2-}$  ions from thiourea in the alkaline solution. The reaction mechanism for CBD can be written as [64, 83, 84]:



Where Cd-salt releases  $\text{Cd}^{2+}$  ions in the cationic precursor solution. In the anionic precursor solution, thiourea hydrolysis provides  $\text{S}^{2-}$  ions according to:



Finally, the CdS are formed by the combination of  $\text{Cd}^{2+}$  and  $\text{S}^{2-}$  ions as:



Controlling the chemical parameters of the solution (e.g., temperature, molar concentration, pH, stirring rate), the thickness of the film and grain size of the particles can be controlled. A proper complexing agent (e.g., ammonium chloride) for CBD improves the homogeneity of the thin films as well as its growth rate. After deposition, the CdS films are removed from the bath and washed ultrasonically to remove loosely adhered CdS particles on the film and finally dried in the air.

## 4. CZTS Solar Cell Device Structure

**4.1. Typical Device Structure.** Mostly used device structure of CZTS thin-film-based solar cell to study the photovoltaic performance has been shown in Figure S2 [85].

Molybdenum-coated soda-lime glass is usually used as an electrical contact. On this Mo-coated substrate, CZTS is deposited as the light absorber layer which is followed by the  $n$ -type CdS layer deposition to form the p-n junction. Next, a thin window layer of transparent conductive oxide

(TCO) (e.g., Al: ZnO, i-ZnO) is formed above the *n*-type layer. Finally, a metal grid (e.g., Al/Ni) is placed on the window layer as an electrical contact. A typical CZTS solar cell device configuration can be expressed as SLG/Mo/CZTS/CdS/Al: ZnO/Al.

**4.2. Using Interfacial Layer.** The implementation of a nanometer-scale interfacial layer to the typical CZTS thin-film solar cell device structure has been found as an efficient way of interface passivation [86]. The thin films grown by atomic layer deposition (ALD) can be deposited on the CZTS absorber layer as shown in Figure S3(a). On the other hand, Figure S3(b) depicts how the interfacial layer (e.g., Al<sub>2</sub>O<sub>3</sub>) can also be laid on the *n*-type CdS layer.

Another remarkable feature of the device structure depicted in Figure S3(b) is that interfacial layer deposited between the absorber layer and the *n*-type layer improves short-circuit current density and fill factor of CZTS solar cell. This improvement results in an overall improvement in cell efficiency. However, above a certain thickness of the interfacial layer, FF and efficiency decrease due to the increased series resistance of the solar cell. Moreover, the deposition of ALD-Al<sub>2</sub>O<sub>3</sub> in the TCO stack results in an average open-circuit voltage enhancement of the CZTS solar cell device [86].

**4.3. Using Fluorine-Doped Tin Oxide (FTO)-Coated Glass Substrate.** FTO conducting substrate is compact having uniform morphology and pleasant interface with CZTS materials [87]. Therefore, the conventional Mo-coated soda-lime glass substrate of the conventional device structure is supplanted by FTO-coated glass substrate [88–90]. Firstly, TCO window layer is deposited on FTO-coated substrate. Secondly, *n*-type CdS layer is deposited on TCO/FTO/glass. Thirdly, the CZTS absorber materials are deposited on the CdS layer. Finally, a metal grid (e.g., Au, Ag, and Mo) is placed on the absorbing layer. Figure S4 is a schematic of the metal grid/CZTS/CdS/FTO/glass configuration of the resulting CZTS thin-film solar cell device structure.

This device structure allows illumination through transparent glass contact. Nevertheless, with the increase of FTO thickness, the transmission of light to the absorbing layer decreases [89]. Notably, the nonohmic contact of the substrate is the primary factor limiting the  $V_{oc}$  and fill factor of the device.

**4.4. Efficiency Roadmap over the Last Decade (2007-2018).** Literature has a copious amount of studies on CZTS-based thin-film solar cells. Since the efficiency of the CZTS-based kesterite structure turned into very low, different approaches have been adopted to enhance the overall performance of the photovoltaic by different compositions of the crystal lattice to be used as an absorber layer. The CZTS-based solar cell technology has made impressive progress over the last decade.

In 1996, the CZTS-based thin film has been constructed for the first time by sulfurization of E-B evaporated precursors, and conversion efficiency was calculated as 0.66% [91]. Conversion efficiency has been gradually increased with the modification of the fabrication process. Later, in the year 2007, Jimbo et al. reported a 5.74% conversion efficiency of

CZTS-type thin-film solar cells using inline-type vacuum apparatus through a multisource evaporation technique [92]. CZTS solar cells were fabricated by Katagiri et al. through the sulfurization method in the next year applying three targets of Cu, SnS, and ZnS by cosputtering technique and 6.77% efficiency was obtained for the first time [93]. In the same year, Friedlmeier et al. investigated CZTSe thin films for the first time achieved an efficiency of about 2% [94]. Later, Zoppi et al. reported that slightly Cu-poor and Zn-rich composition shows a good set of electrical and optical properties of CZTSe material. They fabricated CZTSe thin-film solar cells with the highest 3.2% efficiency in 2009 [95]. On the contrary, initial device performances of CZTSSe thin films were around 0.7%–0.8% [40]. In the year 2010, Todorov et al. fabricated CZTSSe thin-film solar cells with over 9.66% power conversion efficiency for the first time in a hybrid-solution-particle approach [96]. Shin et al. further fabricated selenium-free pure sulfide CZTS using a 150°C vacuum thermal evaporation process and subsequent short high-temperature annealing and reported a cell efficiency of 8.4% in the year 2011 [97]. Later, Repins et al. recorded 9.1% cell efficiency of CZTSe using a vacuum-involved deposition approach allowing real-time control of the composition and reaction path [98]. Aaron et al. studied different Cd-free buffer layers on CZTSSe and achieved an efficiency of 7.6% for In<sub>2</sub>S<sub>3</sub>/CZTSSe solar cells [99]. CZTSSe thin films were further investigated and improved to an efficiency of 11.1% by Yang et al. in the year 2012 using the hydrazine-processed method of fabrication [100]. In 2013, wang et al. reported that the world record efficiency of the CZTSSe cell was reported to be 12.6% [6]. In later days, though Muhunthan et al. [101] and Platzer-Björkman et al. [101, 102] fabricated CZTS in magnetron cosputtering and DC sputtering fabrication methods, respectively, the record-breaking efficiency of 9.2% was achieved by Sun et al. in the year 2016 [103]. They fabricated CZTS thin-film solar cells in sputtering and postsulfurization process on stainless steel substrates using external sodium source. Hong et al., Messaoud et al., and Ericson et al. also fabricated CZTS thin-film solar cells independently in the year 2017 with different buffer layers and each of the research groups achieved efficiencies more than 8.5% [104–106]. Bag et al. reported the Ge substitution in CZTSe solar cells (Sn-Ge alloy with 40% Ge) and obtained an efficiency of 9.14% [107] with an improved open-circuit voltage. Zhou et al. fabricated CZTGeSse thin films using as-synthesized CZTGeS nanocrystals and obtained efficiency beyond 8% [10]. Hages et al. improved the performance further to 9.4% (with 30% of Ge) [108]. To date, the highest performing champion of CZTS-based solar cells (independent of synthesis method) show efficiencies of 10%, 11.6%, and 12.7% for pure sulfur (CZTS), pure selenium (CZTSe), and mixed selenosulfur (CZTSSe) system, respectively [31, 109, 110]. Reported maximum efficiencies of CZTS-based thin-film solar cells are shown in Figure S5.

## 5. Discussions

**5.1. Secondary Phases.** One of the significant challenges to fill the performance difference between CZTS and CIGS solar cells is the formation of secondary phases during the growth and postgrowth processes. The complex and narrow phase

stability makes the challenge more crucial. The chemical potential-based stability diagram is shown in Figure S6 [85]. While varying the potential of Zn and Sn and fixing that of Cu, secondary phases stand along with the CZTS phase [11, 111].

The chemical potential diagram declares that under copper-rich condition (Figure S6a), the CZTS phase is formed within the very narrow red region. The binary (CuS, ZnS, and SnS) and ternary ( $\text{Cu}_2\text{SnS}_3$ ) phases lie on the CZTS phase boundaries under different conditions. Under copper-poor conditions (Figure S6b), CZTS phase clasps into nearly a point that makes CZTS phase formation more complex. Out-diffusion of S at high annealing temperature and unstable nature of Zn and Sn make encouraging conditions to form secondary phases [85]. The properties of secondary phases of CZTS materials are shown in Table 1 [99, 112–114]. ZnS can generate electron-hole pairs and current collection by reducing the active area.  $\text{Cu}_2\text{S}$  may short solar cells because of their high conductivity.  $\text{SnS}_2$  can form secondary diodes inside the CZTS absorber. Its insulating nature could cause high photocarrier recombination. Also,  $\text{Cu}_2\text{SnS}_3$  (CTS) is a ternary compound formed during the growth of CZTS materials under Zn-poor conditions. The efficiency of this material is less than CZTS thin film.

Moreover, other secondary phases such as SnS and  $\text{Sn}_2\text{S}_3$  are also seen in CZTS solar cells, which also hamper solar cell performance. While preparing CZTS thin-film solar cell by CBD-annealing route from SnS/Cu(S)/ZnS, Jianmin et al. [115] identified asymmetric impurity layer of  $\text{SnS}_2$  produced for SnS/CuS/ZnS stack in the annealing process. Thi Hiep Nguyen et al. [53] also reported the formation of  $\text{SnS}_2$  due to the low copper ratio in the composition. With the increase of copper concentration, the  $\text{SnS}_2$  layer disappears, but  $\text{Cu}_2\text{S}$  secondary layer formed instead. Garcia-Llamas et al. [116] also found the relation between the  $\text{Cu}_2\text{S}$  formation and copper ratio in the CZTS thin film composition. They reported that the  $\text{Cu}_2\text{S}$  layer could be eliminated by thermal treatment or controlling Cu-concentration of annealed CZTS thin films. They also found a higher concentration of Sn and S next to Mo back contact for the absorber annealed at a higher heating rate, which results in  $\text{MoS}_2$  and  $\text{MoSn}_2$  secondary phases. Jiahua Tao et al. [117] identified ZnS secondary phase by 325 nm Raman spectra analysis. They also reported that the ZnS layer intensity becomes weak with the increase of copper concentration. Their experimental results show the proximity of the ZnS secondary phase near the surface of CZTS thin films. Jie Ge et al. [14] reported the formation of a SnO<sub>2</sub>-enriched layer due to oxygen segregation. This oxygen segregation varies with the variation of annealing temperature and duration. This eventually varies enrichment of the SnO<sub>2</sub> layer. The secondary phases may form on the CZTS thin film surface, at the Mo/CZTS interface, in bulk, and/or at the grain boundaries. The formation mostly depends on the processing conditions, and it may not be isolated randomly in CZTS thin films. The secondary phases with lower bandgap than CZTS at the metal/CZTS or *n*-type layer/CZTS interface curb open-circuit voltage of solar cells. If the secondary phases in bulk have a wide bandgap, it can reduce the light-absorbing area and eventually decrease the generation of photocarriers. Series

resistance can arise due to secondary phases at the interface. It also reduces the fill factor and short-circuit current.

Postdeposition treatment is necessary to enhance the solar cell device performance. So, controlling the stoichiometry during the postdeposition steps should be studied carefully. Postannealing sulfurization at different temperatures, along with the partial pressure of sulfur, critically controls the distribution of secondary phases and vary the overall device performance [118, 119]. Moreover, at the Mo/CZTS interface molybdenum sulfide ( $\text{MoS}_2$ ) layer is formed, which is a low bandgap indirect semiconductor. The open-circuit voltage of the device can be reduced due to this  $\text{MoS}_2$  formation. Employing an interfacial layer between Mo and CZTS can be a solution to this problem. The intermediate Ag or TiN layer can improve back contact, suppress voids along with secondary phases (e.g.,  $\text{MoS}_2$ ,  $\text{SnS}_2$ ) in the absorber bulk and at the Mo/CZTS interface [120, 121].

**5.2. Defects in CZTS.** Different types of defects, such as vacancies, antisites, and interstitials, exist in CZTS. They cause the formation of shallow donor levels, shallow acceptor levels, mid-gap, and deep level states within the bandgap of the CZTS absorber layer. Zinc and tin vacancies form both mid-gap and deep level states within the bandgap [122, 123], while sulfur vacancies form mid-gap states only. Only copper vacancies are beneficial to CZTS device efficiency as these vacancies enhance the *p*-type material properties of CZTS by forming a shallow acceptor level just above the valence band maxima (VBM). Similar radii of different ionic species are responsible for the formation of antisites defects in CZTS. These antisites defects can form wither acceptor or donor levels in CZTS depending on defect formation energies and their transition levels. Copper and Zinc interstitials are commonly detected in CZTS under copper-rich conditions. They cause shallow donor levels and mid-gap states. That reveals the reason why copper-poor and zinc-rich conditions provide better CZTS solar cell device performance [50]. These antisites and ionization defects cause the local variation of valence band maxima (VBM) and conduction band minima (CBM). The formation of deep-level states, mid-gap states, and donor levels causes the recombination of photogenerated carriers. Shallow donor and/or acceptor defects reduce the optical bandgap and decrease the light absorption of the CZTS absorber layer. High-temperature treatment and doping can play an essential role in defect passivation. Homogenous incorporation of sodium on the CZTS nanocrystal surface can also be a solution to defect passivation [124–126]. However, the minimization of defects while growing the CZTS thin-film device is vital to achieving a high-performance solar cell device.

**5.3. Electrical and Optical Properties.** The electronic band structure of kesterite CZTS, along with two symmetry directions (110) and (001), is seen in Figure S7 [117]. The energy is referred to as the valence band maxima (VBM), and spin-orbit interaction is also included. The lowest conduction band and the topmost valence band have relatively flat band dispersions.

TABLE 1: Various properties of secondary phases observed in CZTS materials.

Properties	ZnS	Cu <sub>2</sub> S	SnS <sub>2</sub>	Cu <sub>2</sub> SnS <sub>3</sub>
Band gap	3.54-3.68 eV	1.21 eV	2.2 eV	<b>0.98-1.35 eV</b>
Electrical properties	Insulator	<i>p</i> -type, highly defective	<i>n</i> -type	<i>p</i> -type
Structural properties	Sphalerite and wurtzite	Chalcocite	Rhombohedral	Cubic and tetragonal
Impact on solar cell performance	Reduces device active area	Metallic and short the solar cell	Forms diodes also, barriers for carrier collection	Affects carrier collection efficiency

The theoretically measured bandgap of CZTS is within 1.4-1.6 eV range that has been justified by experiments also. This bandgap is close to the optimum bandgap required for thin-film solar cells. The bandgap indicates CZTS as a promising absorber material for thin-film solar cell applications. The bandgap of the CZTS material shifts to higher energies with the decrease of the Cu/(Zn+Sn) ratio. Moreover, CZTS material has a high absorbance of light in the visible region of the spectrum. The absorption coefficient has been found larger than  $10^4 \text{ cm}^{-1}$  in this visible range [127], which supports the direct bandgap nature of the material.

However, C. Persson demonstrated by the density of states shown in Figure S8 [117] that in the lower energy region, the valence band density of states contains hybridization of Cu-d and anion-p, Zn-sp<sub>d</sub>, Cu-s, and Sn-p. The conduction band density of states contains hybridization of cation-s anion and anion-p. Having strong Sn-s and anion-p in the lowest conduction band is a very characteristic property of CZTS material.

Figure S9 shows the absorption spectra of Cu<sub>2</sub>ZnSn(S<sub>x</sub>Se<sub>1-x</sub>)<sub>4</sub> powder. The CZTSSe nanocrystals have high optical absorptions from the visible to the near-infrared spectrum. The bandgap energy can be determined from the absorption spectra. The bandgap energy usually varies between 1 and 1.5 eV almost linearly. The lowest energy absorption peak is related to the bandgap of the material. The peak shifts toward shorter wavelength with the increase of bandgap [128]. The optical absorption spectra of CZTS material is also a function of its average diameter [129]. Both the edge of the optical absorption spectra and the lowest energy absorption peak are inversely proportional to nanocrystal diameter.

Furthermore, the effective mass of minority carriers of CZTS is more massive than that of CIGS material. This is a disadvantage of using this indium-free *p*-type absorbing layer. The effective hole masses show strong anisotropy. The refractive index and dielectric constant of semiconducting materials are significant for designing solar cell devices. The refractive index and optical static dielectric constants are found to be around 2.85 and 13.653, respectively. The optical high-frequency dielectric constant is usually within 8.2-8.45 [110].

**5.4. Challenges and Future Prospects.** The highest efficiency reported for CZTS based solar cells is 12.6% with  $V_{oc} = 0.51 \text{ V}$ ,  $J_{sc} = 35.2 \text{ mA/cm}^2$ , and  $FF = 69.8\%$  [6]. Compared to the best performance of CIGS solar cells, the focus should be given to open-circuit voltage and fill factor of CZTS solar cell

technology. Earth abundance, nontoxicity, and cost-effectiveness have made CZTS a promising material to compete for CIGS technology. However, the presence of secondary phases and defects result in many challenges for CZTS technology. It has become a challenging issue to detect secondary phases applying present techniques because of similar crystal structures of many secondary phases with CZTS. Moreover, a tiny amount of defect concentration present in the CZTS absorber layer is well enough to cause poor device performance. Novel growth and characterization techniques, interface engineering, and deeper understanding of defects and secondary phases should be given further attention for the further improvement of CZTS solar cell efficiency.

Novel material growth techniques are required to detect and avoid secondary phases and defects. The development of effective defect passivation and surface passivation along with novel synthesis technique approach for CZTS can reduce the unwanted secondary phases and increase the beneficial defects and grain boundary defects. Moreover, many present characterization techniques are inadequate to detect the secondary phases and defects in the CZTS absorbing layer. Development of the characterization approach to precisely find the 3D distribution of stoichiometry will be a vital tool to identify and correlate variations and defects in the local stoichiometry. This will help to get rid of the local inconsistency in the open-circuit voltage and carrier concentration. The focus should also be given on interface optimization for bandgap alignment and efficient carrier transportation. The interface within the absorber, between grains and grain boundaries, can be engineered to reduce carrier combination. The sizeable positive spike at the CZTS/CdS interface reduces the short-circuit current density, and the negative spike at the interface is responsible for reduces open-circuit voltage. So, developing an alternative interfacial layer will be able to overcome these shortcomings. The growth of secondary phases along with voids near the Mo interface further reduces open-circuit voltage and short-circuit current. This issue can also be solved by modifying or replacing existing interfaces with new efficient carrier transport interface materials.

## 6. Conclusion

The unique features of CZTS thin film have made this material an auspicious research topic in recent years. However, comparatively low conversion efficiency, expensive manufacturing equipment, complicated process steps, and low earnings show that there is still a long way to go. It is

crucial to understand the formation mechanism of CZTS thoroughly to achieve high performance. The knowledge of controlling dynamic material growth and detecting unwanted secondary phases and defects will help to overcome the performance gap between CZTS and CIGS solar cells. In this work, we strategically reviewed CZTS and CdS synthesis techniques, CZTS solar cell device structures, electrical and optical properties, and secondary phases in the earth-abundant CZTS absorbing layer. The present status of CZTS technology and common synthesis technologies are discussed to help the researchers to focus on their prospects on more appropriate material growth techniques for large-scale production of CZTS solar cells along with easy control over material characterization.

In short, further development of synthesis technology and equipment, as well as substantial theoretical research and understanding, will turn CZTS thin film a promising photovoltaic material after the CIGS material.

### Conflicts of Interest

The author declares that there is no conflict of interest regarding the publication of this paper.

### Supplementary Materials

Figure S1: Crystal structure of (a) stannite and (b) kesterite CZTS [1]. Figure S2: Typical device structure for CZTS solar cells (adapted from [2]). Figure S3: Schematic of device structures with Al<sub>2</sub>O<sub>3</sub> on the top of (a) Absorber layer (b) *n*-type CdS layer (adapted from [3]). Figure S4: Schematic of CZTS device structures with FTO coated Substrate. Figure S5: Improvement of conversion efficiency on CZTS-based thin-film solar cells ([4]–[23]). Figure S6: Chemical potential based stability diagram for tin and zinc under (a) copper-rich and (b) copper-poor conditions.  $\Delta\mu$  is the chemical potential for the standard element. (adapted from [2]). Figure S7: Electronic band structure of kesterite CZTS along with the two symmetry directions (110) and (001) (adapted from [24]). Figure S8: Atomic resolved DOS of CZTS, presented with a 0.1 eV Lorentzian broadening. The gray area in the upper panels represents the DOS of Cu atoms, and the thick blue line represents Zn atoms. In the lower panels, the gray area represents S, and the thick blue line represents Sn atoms (adapted from [25]). Figure S9: Absorption spectra of Cu<sub>2</sub>ZnSn(S<sub>x</sub>Se<sub>1-x</sub>)<sub>4</sub> powders (adapted from [26]). (Supplementary Materials)

### References

- [1] X. Song, X. Ji, M. Li, W. Lin, X. Luo, and H. Zhang, "A review on development prospect of CZTS based thin film solar cells," *International Journal of Photoenergy*, vol. 2014, Article ID 613173, 11 pages, 2014.
- [2] M. P. Suryawanshi, G. L. Agawane, S. M. Bhosale et al., "CZTS based thin film solar cells: a status review," *Materials Technology*, vol. 28, no. 1-2, pp. 98–109, 2013.
- [3] P. Jackson, R. Wuerz, D. Hariskos, E. Lotter, W. Witte, and M. Powalla, "Effects of heavy alkali elements in Cu(In,Ga)-Se<sub>2</sub>solar cells with efficiencies up to 22.6%," *Physica Status Solidi (RRL) - Rapid Research Letters*, vol. 10, no. 8, pp. 583–586, 2016.
- [4] H. A. Atwater and A. Polman, "Erratum: Plasmonics for improved photovoltaic devices," *Nature Materials*, vol. 9, no. 10, p. 865, 2010.
- [5] M. Green, K. Emery, Y. Hishikawa, W. Warta, and E. Dunlop, "Solar cell efficiency tables (version 54)," *Progress in Photovoltaics: Research and Applications*, vol. 21, no. 1, 2013.
- [6] W. Wang, M. T. Winkler, O. Gunawan et al., "Device Characteristics of CZTSSe Thin-Film Solar Cells with 12.6% Efficiency," *Advanced Energy Materials*, vol. 4, no. 7, 2014.
- [7] X. Wang, W. Song, B. Liu et al., "High-Performance Organic-Inorganic Hybrid Photodetectors Based on P3HT:CdSe Nanowire Heterojunctions on Rigid and Flexible Substrates," *Advanced Functional Materials*, vol. 23, no. 9, pp. 1202–1209, 2013.
- [8] L. M. Peter, "Towards sustainable photovoltaics: The search for new materials," *Philosophical Transactions of the Royal Society A: Mathematical, Physical and Engineering Sciences*, vol. 369, no. 1942, pp. 1840–1856, 2011.
- [9] A. Lafond, C. Guillot-Deudon, J. Vidal, M. Paris, C. La, and S. Jobic, "Substitution of Li for Cu in Cu<sub>2</sub>ZnSnS<sub>4</sub>: Toward Wide Band Gap Absorbers with Low Cation Disorder for Thin Film Solar Cells," *Inorganic Chemistry*, vol. 56, no. 5, pp. 2712–2721, 2017.
- [10] H. Zhou, W. C. Hsu, H. S. Duan et al., "CZTS nanocrystals: a promising approach for next generation thin film photovoltaics," *Energy & Environmental Science*, vol. 6, no. 10, pp. 2822–2838, 2013.
- [11] S. Chen, X. G. Gong, A. Walsh, and S. H. Wei, "Defect Physics of the Kesterite Thin-Film Solar Cell Absorber Cu<sub>2</sub>ZnSnS<sub>4</sub>," *Applied Physics Letters*, vol. 96, no. 2, p. 021902, 2010.
- [12] S. Chen, J. H. Yang, X. G. Gong, A. Walsh, and S. H. Wei, "Intrinsic Point Defects and Complexes in the Quaternary Kesterite semiconductor Cu<sub>2</sub>ZnSnS<sub>4</sub>," *Physical Review B*, vol. 81, no. 24, 2010.
- [13] D. Han, Y. Y. Sun, J. Bang et al., "Deep Electron Traps and Origin of *off*-type Conductivity in the Earth-Abundant Solar-Cell Material Cu<sub>2</sub>ZnSnS<sub>4</sub>," *Physical Review B*, vol. 87, no. 15, 2013.
- [14] J. Ge, Y. Yu, W. Ke et al., "Improved Performance of Electroplated CZTS Thin-Film Solar Cells with Bifacial Configuration," *ChemSusChem*, vol. 9, no. 16, pp. 2149–2158, 2016.
- [15] A. Jain, S. P. Ong, G. Hautier et al., "Commentary: The Materials Project: a materials genome approach to accelerating materials innovation," *APL Materials*, vol. 1, no. 1, 2013.
- [16] R. Hoffman, "Materials for CZTS photovoltaic devices," in *The NNIN REU Research Accomplishments*, Chemical Engineering, Cornell University, 2009.
- [17] G. K. Dalapati, S. Masudy-Panah, A. Kumar, C. C. Tan, H. R. Tan, and D. Chi, "Aluminium alloyed iron-silicide/silicon solar cells: a simple approach for low cost environmental-friendly photovoltaic technology," *Scientific Reports*, vol. 5, no. 1, 2016.
- [18] G. K. Dalapati, S. Masudy-Panah, S. T. Chua et al., "Color Tunable Low Cost Transparent Heat Reflector Using Copper and Titanium Oxide for Energy Saving Application," *Scientific Reports*, vol. 6, no. 1, 2016.
- [19] N. Selvakumar and H. C. Barshilia, "Review of physical vapor deposited (PVD) spectrally selective coatings for mid- and

- high-temperature solar thermal applications,” *Solar Energy Materials and Solar Cells*, vol. 98, pp. 1–23, 2012.
- [20] N. Selvakumar, A. Biswas, K. Rajaguru, G. M. Gouda, and H. C. Barshilia, “Nanometer thick tunable AlHfN coating for solar thermal applications: transition from absorber to antireflection coating,” *Solar Energy Materials & Solar Cells*, vol. 137, pp. 219–226, 2015.
- [21] S. Masudy-Panah, K. Radhakrishnan, H. R. Tan, R. Yi, T. I. Wong, and G. K. Dalapati, “Titanium doped cupric oxide for photovoltaic application,” *Solar Energy Materials & Solar Cells*, vol. 140, pp. 266–274, 2015.
- [22] S. Masudy-Panah, R. Siavash Moakhar, C. S. Chua et al., “Nanocrystal engineering of sputter-grown CuO photocathode for visible-light-driven electrochemical water splitting,” *ACS Applied Materials & Interfaces*, vol. 8, no. 2, pp. 1206–1213, 2016.
- [23] D. H. Son, D. H. Kim, K. J. Yang et al., “Influence of Precursor Sulfur Content on Film Formation and the Properties of Sulfurized  $\text{Cu}_2\text{ZnSnS}_4$  thin Films for Solar Cells,” *Physica Status Solidi (A) Applications and Materials Science*, vol. 211, no. 4, pp. 946–951, 2014.
- [24] M. G. Sousa, A. F. Da Cunha, P. M. P. Salomé, P. A. Fernandes, J. P. Teixeira, and J. P. Leitão, “ $\text{Cu}_2\text{ZnSnS}_4$  absorber layers obtained through sulphurization of metallic precursors: graphite box versus Sulphur flux,” in *Thin Solid Films*, vol. 535, pp. 27–30, 2013.
- [25] M. Abusnina, H. Moutinho, M. Al-Jassim, C. Dehart, and M. Matin, “Fabrication and Characterization of CZTS Thin Films Prepared by the Sulfurization of RF-Sputtered Stacked Metal Precursors,” *Journal of Electronic Materials*, vol. 43, no. 9, pp. 3145–3154, 2014.
- [26] M. G. Gang, K. V. Gurav, S. W. Shin et al., “A 5.1% efficient kesterite  $\text{Cu}_2\text{ZnSnS}_4$  (CZTS) thin film solar cell prepared using modified sulfurization process,” *Physica Status Solidi*, vol. 12, no. 6, pp. 713–716, 2015.
- [27] M. Abusnina, M. Matin, H. R. Moutinho et al., “Suppression of the  $\text{Cu}_{2-x}\text{S}$  secondary phases in CZTS films through controlling the film elemental composition,” *IEEE Journal of Photovoltaics*, vol. 5, no. 5, pp. 1470–1475, 2015.
- [28] H. Sugimoto, C. Liao, H. Hiroi, N. Sakai, and T. Kato, “Lifetime improvement for high efficiency  $\text{Cu}_2\text{ZnSnS}_4$  submodules,” in *Photovoltaic Specialists Conference (PVSC), 2013 IEEE 39th*, pp. 3208–3211, Tampa, FL, USA, June 2013.
- [29] S. M. Pawar, A. I. Inamdar, B. S. Pawar et al., “Synthesis of  $\text{Cu}_2\text{ZnSnS}_4$  (CZTS) Absorber by Rapid Thermal Processing (RTP) Sulfurization of Stacked Metallic Precursor Films for Solar Cell Applications,” *Materials Letters*, vol. 118, pp. 76–79, 2014.
- [30] Y. Feng, B. Yu, G. Cheng et al., “Searching for a Fabrication Route of Efficient  $\text{Cu}_2\text{ZnSnS}_4$  solar Cells by Post-Sulfuration of Co-Sputtered Sn-Enriched Precursors,” *Journal of Materials Chemistry C*, vol. 3, no. 37, pp. 9650–9656, 2015.
- [31] K. Sun, C. Yan, F. Liu et al., “Over 9% Efficient Kesterite  $\text{Cu}_2\text{ZnSnS}_4$  Solar Cell Fabricated by Using  $\text{Zn}_{1-x}\text{Cd}_x\text{S}$  Buffer Layer,” *Advanced Energy Materials*, vol. 6, no. 12, 2016.
- [32] B. T. Jheng, P. T. Liu, M. C. Wang, and M. C. Wu, “Effects of ZnO-Nanostructure Antireflection Coatings on Sulfurization-Free  $\text{Cu}_2\text{ZnSnS}_4$  absorber Deposited by Single-Step Co-Sputtering Process,” *Applied Physics Letters*, vol. 103, no. 5, p. 052904, 2013.
- [33] N. Momose, M. T. Htay, T. Yudasaka et al., “ $\text{Cu}_2\text{ZnSnS}_4$  Thin film solar cells utilizing sulfurization of metallic precursor prepared by simultaneous sputtering of metal targets,” *Japanese Journal of Applied Physics*, vol. 50, p. 01BG09, 2011.
- [34] Y. Feng, T. K. Lau, G. Cheng et al., “A low-temperature formation path toward highly efficient se-free  $\text{Cu}_2\text{ZnSnS}_4$  solar cells fabricated through sputtering and sulfurization,” *CrytEngComm*, vol. 18, no. 6, pp. 1070–1077, 2016.
- [35] J. J. Scragg, T. Ericson, X. Fontané et al., “Rapid Annealing of Reactively Sputtered Precursors for  $\text{Cu}_2\text{ZnSnS}_4$  solar Cells,” *Progress in Photovoltaics: Research and Applications*, vol. 22, no. 1, pp. 10–17, 2014.
- [36] P.-A. Cormier and R. Snyders, “One-step synthesis of  $\text{Cu}_2\text{ZnSnS}_4$  thin films by reactive magnetron co-sputtering,” *Acta Materialia*, vol. 96, pp. 80–88, 2015.
- [37] R. Nakamura, K. Tanaka, H. Uchiki, K. Jimbo, T. Washio, and H. Katagiri, “ $\text{Cu}_2\text{ZnSnS}_4$  thin Film Deposited by Sputtering with  $\text{Cu}_2\text{ZnSnS}_4$  compound Target,” *Japanese Journal of Applied Physics*, vol. 53, no. 2S, article 02BC10, 2014.
- [38] B. T. Jheng, K. M. Huang, S. F. Chen, and M. C. Wu, “Effects of Substrate Temperature on the  $\text{Cu}_2\text{ZnSnS}_4$  films Deposited by Radio-Frequency Sputtering with Single Target,” *Thin Solid Films*, vol. 564, pp. 345–350, 2014.
- [39] Y. Kim, K. Woo, I. Kim, Y. S. Cho, S. Jeong, and J. Moon, “Highly concentrated synthesis of copper-zinc-tin-sulfide nanocrystals with easily decomposable capping molecules for printed photovoltaic applications,” *Nanoscale*, vol. 5, no. 21, pp. 10183–10188, 2013.
- [40] Q. Guo, H. W. Hillhouse, and R. Agrawal, “Synthesis of  $\text{Cu}_2\text{ZnSnS}_4$  nanocrystal ink and its use for solar cells,” *Journal of the American Chemical Society*, vol. 131, no. 33, pp. 11672–11673, 2009.
- [41] Q. Guo, G. M. Ford, W. C. Yang et al., “Fabrication of 7.2% efficient CZTSSe solar cells using CZTS nanocrystals,” *Journal of the American Chemical Society*, vol. 132, no. 49, pp. 17384–17386, 2010.
- [42] Y. Cao, M. S. Denny Jr., J. V. Caspar et al., “High-efficiency solution-processed  $\text{Cu}_2\text{ZnSn}(\text{S},\text{Se})_4$  thin-film solar cells prepared from binary and ternary nanoparticles,” *Journal of the American Chemical Society*, vol. 134, no. 38, pp. 15644–15647, 2012.
- [43] K. Sekiguchi, M. Shimizu, and H. Miyajima, “Quantized  $e^2/h$  Step and Nonquantized Step in Nanocontact Magnetoresistance,” *IEEE Transactions on Magnetics*, vol. 42, no. 10, pp. 2618–2620, 2006.
- [44] K. Sekiguchi, K. Tanaka, K. Moriya, and H. Uchiki, “Epitaxial growth of  $\text{Cu}_2\text{ZnSnS}_4$  thin films by pulsed laser deposition,” *Physica Status Solidi (C) Current Topics in Solid State Physics*, vol. 3, no. 8, pp. 2618–2621, 2006.
- [45] K. Moriya, K. Tanaka, and H. Uchiki, “Fabrication of  $\text{Cu}_2\text{ZnSnS}_4$  Thin-Film solar cell prepared by pulsed laser deposition,” *Japanese Journal of Applied Physics*, vol. 46, no. 9A, pp. 5780–5781, 2007.
- [46] L. Sun, J. He, Y. Chen, F. Yue, P. Yang, and J. Chu, “Comparative study on  $\text{Cu}_2\text{ZnSnS}_4$  thin films deposited by sputtering and pulsed laser deposition from a single quaternary sulfide target,” *Journal of Crystal Growth*, vol. 361, pp. 147–151, 2012.
- [47] B. Long, S. Cheng, Q. Zheng, J. Yu, and H. Jia, “Effects of Sulfurization Time and  $\text{H}_2\text{S}$  Concentration on Electrical

- Properties of  $\text{Cu}_2\text{ZnSnS}_4$  Films Prepared by Sol-Gel Method,” *Materials Research Bulletin*, vol. 73, pp. 140–144, 2016.
- [48] L. Dong, S. Cheng, Y. Lai, H. Zhang, and H. Jia, “Sol-Gel Processed CZTS Thin Film Solar Cell on Flexible Molybdenum Foil,” *Thin Solid Films*, vol. 626, pp. 168–172, 2017.
- [49] Y. Miyamoto, K. Tanaka, M. Oonuki, N. Moritake, and H. Uchiki, “Optical Properties of  $\text{Cu}_2\text{ZnSnS}_4$  Thin Films Prepared by Sol-Gel and Sulfurization Method,” *Japanese Journal of Applied Physics*, vol. 47, no. 1, pp. 596–597, 2008.
- [50] K. Tanaka, M. Oonuki, N. Moritake, and H. Uchiki, “ $\text{Cu}_2\text{ZnSnS}_4$  thin film solar cells prepared by non-vacuum processing,” *Solar Energy Materials & Solar Cells*, vol. 93, no. 5, pp. 583–587, 2009.
- [51] K. Tanaka, Y. Fukui, N. Moritake, and H. Uchiki, “Chemical composition dependence of morphological and optical properties of  $\text{Cu}_2\text{ZnSnS}_4$  thin films deposited by sol-gel sulfurization and  $\text{Cu}_2\text{ZnSnS}_4$  thin film solar cell efficiency,” *Solar Energy Materials & Solar Cells*, vol. 95, no. 3, pp. 838–842, 2011.
- [52] R. Moreno, E. A. Ramirez, and G. Gordillo Guzmán, “Study of optical and structural properties of CZTS thin films grown by co-evaporation and spray pyrolysis,” *Journal of Physics: Conference Series*, vol. 687, no. 1, article 012041, 2016.
- [53] T. H. Nguyen, T. Harada, S. Nakanishi, and S. Ikeda, “ $\text{Cu}_2\text{ZnSnS}_4$ -based thin film solar cells with more than 8% conversion efficiency obtained by using a spray pyrolysis technique,” in *2017 IEEE 44th Photovoltaic Specialist Conference, PVSC 2017*, pp. 470–472, Portland, OR, USA, June 2016.
- [54] J. J. Scragg, P. J. Dale, L. M. Peter, G. Zoppi, and I. Forbes, “New routes to sustainable photovoltaics: evaluation of  $\text{Cu}_2\text{ZnSnS}_4$  as an alternative absorber material,” *Physica Status Solidi*, vol. 245, no. 9, pp. 1772–1778, 2008.
- [55] J. J. Scragg, D. M. Berg, and P. J. Dale, “A 3.2% efficient Kesterite device from electrodeposited stacked elemental layers,” *Journal of Electroanalytical Chemistry*, vol. 646, no. 1-2, pp. 52–59, 2010.
- [56] A. Ennaoui, M. Lux-Steiner, A. Weber et al., “ $\text{Cu}_2\text{ZnSnS}_4$  thin film solar cells from electroplated precursors: Novel low-cost perspective,” *Thin Solid Films*, vol. 517, no. 7, pp. 2511–2514, 2009.
- [57] R. Schurr, A. Hölzing, S. Jost et al., “The Crystallisation of  $\text{Cu}_2\text{ZnSnS}_4$  thin Film Solar Cell Absorbers from Co-Electroplated cu-Zn-Sn Precursors,” *Thin Solid Films*, vol. 517, no. 7, pp. 2465–2468, 2009.
- [58] H. Araki, Y. Kubo, A. Mikaduki et al., “Preparation of  $\text{Cu}_2\text{ZnSnS}_4$  thin films by sulfurizing electroplated precursors,” *Solar Energy Materials and Solar Cells*, vol. 93, no. 6-7, pp. 996–999, 2009.
- [59] S. Ahmed, K. B. Reuter, O. Gunawan, L. Guo, L. T. Romaniki, and H. Deligianni, “A High Efficiency Electrodeposited  $\text{Cu}_2\text{ZnSnS}_4$  Solar Cell,” *Advanced Energy Materials*, vol. 2, no. 2, pp. 253–259, 2012.
- [60] J. Zhang, L. Sun, C. Liao, and C. Yan, “Size Control and Photoluminescence Enhancement of CdS Nanoparticles Prepared Via Reverse Micelle Method,” *Solid State Communications*, vol. 124, no. 1-2, pp. 45–48, 2002.
- [61] L. Q. Pham, T. K. Van, H. G. Cha, and Y. S. Kang, “Controlling crystal growth orientation and crystallinity of cadmium sulfide nanocrystals in aqueous phase by using cationic surfactant,” *CrystEngComm*, vol. 14, no. 23, pp. 7888–7890, 2012.
- [62] A. Pal, J. Dutta, D. Bhattacharyya, S. Chaudhuri, and A. K. Pal, “Electrodeposited CdTe Films: Space Charge Limited Conduction,” *Vacuum*, vol. 46, no. 2, pp. 147–150, 1995.
- [63] S. J. Castillo, A. Mendoza-Galván, R. Ramírez-Bon et al., “Structural, Optical and Electrical Characterization of in/CdS/Glass Thermally Annealed System,” *Thin Solid Films*, vol. 373, no. 1-2, pp. 10–14, 2000.
- [64] M. A. Islam, M. S. Hossain, M. M. Aliyu et al., “Comparison of structural and optical properties of CdS thin films grown by CSVT, CBD and sputtering techniques,” *Energy Procedia*, vol. 33, pp. 203–213, 2013.
- [65] X. Liu, J. Chen, M. Luo et al., “Thermal evaporation and characterization of  $\text{Sb}_2\text{Se}_3$  Thin film for substrate  $\text{Sb}_2\text{Se}_3/\text{CdS}$  solar cells,” *ACS Applied Materials & Interfaces*, vol. 6, no. 13, pp. 10687–10695, 2014.
- [66] L. C. Kuo, C. Y. Shei, W. Y. Hsu, Y. T. Tsai, and J. H. Kung, “The effect of sintering conditions on screen-printed CdS films,” in *Conference Record of the Twenty Third IEEE Photovoltaic Specialists Conference -1993 (Cat. No.93CH3283-9)*, pp. 539–542, Louisville, KY, USA, USA, May 1993.
- [67] S. Ikegami, “CdS/CdTe solar cells by the screen-printing-sintering technique: Fabrication, photovoltaic properties and applications,” *Solar Cells*, vol. 23, no. 1-2, pp. 89–105, 1988.
- [68] M. A. Mahdi, S. J. Kasem, J. J. Hassen, and A. A. Swadi, “Structural and optical properties of chemical deposition CdS thin films,” *International Journal of Nanoelectronics and Materials (IJNeAM)*, vol. 2, no. 2, pp. 163–172, 2009.
- [69] G. A. Somorjai and D. W. Jepsen, “Evaporation Mechanism of CdS Single Crystals. I. Surface Concentration and Temperature Dependence of the Evaporation Rate,” *The Journal of Chemical Physics*, vol. 41, no. 5, pp. 1389–1393, 1964.
- [70] C. M. Dai, L. Horng, W. F. Hsieh, Y. T. Shih, C. T. Tsai, and D. S. Chuu, “High orientation CdS thin films grown by pulsed laser and thermal evaporation,” *Journal of Vacuum Science and Technology A*, vol. 10, no. 3, pp. 484–488, 1992.
- [71] N. Memarian, M. S. Rozati, I. Concina, and A. Vomiero, “Deposition of Nanostructured CdS Thin Films by Thermal Evaporation Method: Effect of Substrate Temperature,” *Materials*, vol. 10, no. 7, p. 773, 2017.
- [72] W. Lee, J. Sharp, G. A. Umana-Membreno, J. Dell, and L. Faraone, “Deposition heating effect on CdS thin films prepared by thermal evaporation for CdTe solar cells,” in *2014 Conference on Optoelectronic and Microelectronic Materials & Devices*, pp. 153–155, Perth, WA, Australia, Dec. 2014.
- [73] F. A. Pizzarello, “CdS thin-film formation by the method of co-evaporation,” *Journal of Applied Physics*, vol. 35, no. 9, pp. 2730–2732, 1964.
- [74] H. S. Kwok, J. P. Zheng, S. Witanachchi et al., “Growth of highly oriented CdS thin films by laser-evaporation deposition,” *Applied Physics Letters*, vol. 52, no. 13, pp. 1095–1097, 1988.
- [75] Y. Y. Ma, A. L. Fahrenbruch, and R. H. Bube, “Photovoltaic properties of n-CdS/p-CdTe heterojunctions prepared by spray pyrolysis,” *Applied Physics Letters*, vol. 30, no. 8, pp. 423–424, 1977.
- [76] Y. Y. Ma and R. H. Bube, “Properties of CdS Films Prepared by Spray Pyrolysis,” *Journal of The Electrochemical Society*, vol. 124, no. 9, p. 1430, 1977.

- [77] A. Ashour, "Physical Properties of Spray Pyrolysed CdS Thin Films," *Turkish Journal of Physics*, vol. 27, no. 6, pp. 551–558, 2003.
- [78] V. Bilgin, S. Kose, F. Atay, and I. Akyuz, "The Effect of Substrate Temperature on the Structural and some Physical Properties of Ultrasonically Sprayed CdS Films," *Materials Chemistry and Physics*, vol. 94, no. 1, pp. 103–108, 2005.
- [79] V. Kumar, S. Juneja, S. K. Sharma, V. Singh, and T. P. Sharma, "Optimization of Sintering Temperature in CdZnS Films Using Reflection Spectroscopy," *Journal of Coatings Technology and Research*, vol. 7, no. 3, pp. 399–402, 2010.
- [80] V. Kumar, J. K. Gaur, M. K. Sharma, and T. P. Sharma, "Electrical properties of cadmium telluride screen-printed films for photovoltaic applications," *Chalcogenide Letters*, vol. 5, no. 8, pp. 171–176, 2008.
- [81] T. Arita, A. Hanafusa, N. Ueno, Y. Nishiyama, S. Kitamura, and M. Murozono, "CdS/CdTe solar cells with improved CdS films fabricated by the writing method," *Solar Energy Materials*, vol. 23, no. 2-4, pp. 371–379, 1991.
- [82] V. Kumar, D. K. Sharma, M. K. Bansal, D. K. Dwivedi, and T. P. Sharma, "Synthesis and characterization of screen-printed CdS films," *Science of Sintering*, vol. 43, no. 3, pp. 335–341, 2011.
- [83] Y. A. Kalandaragh, M. B. Muradov, R. K. Mamedov, M. Behboudnia, and A. Khodayari, "Structural, compositional and optical characterization of water soluble CdS nanoparticles synthesized by ultrasonic irradiation," *Optoelectronics and Advanced Materials - Rapid Communications*, vol. 2, no. 1, p. 42, 2003.
- [84] A. J. Haider, A. M. Mousa, and S. M. Al-Jawad, "Annealing effect on structural, electrical and optical properties of CdS films prepared by CBD method," *Journal of Semiconductor Technology and Science*, vol. 8, no. 4, pp. 326–332, 2008, [http://scholar.googleusercontent.com/scholar?q=cache:KYvyFHVZctEJ:scholar.google.com/+Haider,+A.+J.,+Mousa,+A.+M.,+%26+Al-Jawad,+S.+M.+\(2008\).+Annealing+effect+on+structural,+electrical+and+optical+properties+of+CdS+films+prepared+by+CBD+method.+Journal+o](http://scholar.googleusercontent.com/scholar?q=cache:KYvyFHVZctEJ:scholar.google.com/+Haider,+A.+J.,+Mousa,+A.+M.,+%26+Al-Jawad,+S.+M.+(2008).+Annealing+effect+on+structural,+electrical+and+optical+properties+of+CdS+films+prepared+by+CBD+method.+Journal+o)
- [85] M. Kumar, A. Dubey, N. Adhikari, S. Venkatesan, and Q. Qiao, "Strategic Review of Secondary Phases, Defects and Defect-Complexes in Kesterite CZTS-se Solar Cells," *Energy & Environmental Science*, vol. 8, no. 11, pp. 3134–3159, 2015.
- [86] Y. S. Lee, T. Gershon, T. K. Todorov et al., "Atomic Layer Deposited Aluminum Oxide for Interface Passivation of  $\text{Cu}_2\text{ZnSn}(\text{S},\text{Se})_4$  Thin-Film Solar Cells," *Advanced Energy Materials*, vol. 6, no. 12, 2016.
- [87] J. S. Kim, J. K. Kang, and D. K. Hwang, "High efficiency bifacial  $\text{Cu}_2\text{ZnSnS}_4$  thin-film solar cells on transparent conducting oxide glass substrates," *APL Mater*, vol. 4, no. 9, article 096101, 2016.
- [88] R. Chen, J. Fan, C. Liu, X. Zhang, Y. Shen, and Y. Mai, "Solution-Processed One-Dimensional  $\text{ZnO}@\text{CdS}$  Heterojunction toward Efficient  $\text{Cu}_2\text{ZnSnS}_4$  Solar Cell with Inverted Structure," *Scientific Reports*, vol. 6, no. 1, 2016.
- [89] N. E. Gorji, "Quantitative Analysis of the Optical Losses in CZTS Thin-Film Semiconductors," *IEEE Transactions on Nanotechnology*, vol. 13, no. 4, pp. 743–748, 2014.
- [90] S. Mahajan, E. Stathatos, N. Huse, R. Birajdar, A. Kalarakis, and R. Sharma, "Low Cost Nanostructure Kesterite CZTS Thin Films for Solar Cells Application," *Materials Letters*, vol. 210, pp. 92–96, 2018.
- [91] H. Katagiri and K. Jimbo, "Development of rare metal-free CZTS-based thin film solar cells," in *2011 37th IEEE Photovoltaic Specialists Conference*, pp. 3516–3521, Seattle, WA, USA, Jun 2011.
- [92] K. Jimbo, R. Kimura, T. Kamimura et al., " $\text{Cu}_2\text{ZnSnS}_4$ -Type Thin Film Solar Cells Using Abundant Materials," *Thin Solid Films*, vol. 515, no. 15, pp. 5997–5999, 2007.
- [93] H. Katagiri, K. Jimbo, S. Yamada et al., "Enhanced Conversion Efficiencies of  $\text{Cu}_2\text{ZnSnS}_4$ -Based Thin Film Solar Cells by Using Preferential Etching Technique," *Applied Physics Express*, vol. 1, p. 041201, 2008.
- [94] G. Suresh Babu, Y. B. Kishore Kumar, P. Uday Bhaskar, and V. Sundara Raja, "Growth and Characterization of Co-Evaporated  $\text{Cu}_2\text{ZnSnS}_4$  thin Films for Photovoltaic Applications," *Journal of Physics D: Applied Physics*, vol. 41, no. 20, p. 205305, 2008.
- [95] G. Zoppi, I. Forbes, R. W. Miles, P. J. Dale, J. J. Scragg, and L. M. Peter, " $\text{Cu}_2\text{ZnSnSe}_4$  thin Film Solar Cells Produced by Selenisation of Magnetron Sputtered Precursors," *Progress in Photovoltaics: Research and Applications*, vol. 17, no. 5, pp. 315–319, 2009.
- [96] T. K. Todorov, K. B. Reuter, and D. B. Mitzi, "High-Efficiency Solar Cell with Earth-Abundant Liquid-Processed Absorber," *Advanced Materials*, vol. 22, no. 20, pp. E156–E159, 2010.
- [97] B. Shin, O. Gunawan, Y. Zhu, N. A. Bojarczuk, S. J. Chey, and S. Guha, "Thin Film Solar Cell with 8.4% Power Conversion Efficiency Using an Earth-Abundant  $\text{Cu}_2\text{ZnSnS}_4$  absorber," *Progress in Photovoltaics: Research and Applications*, vol. 21, no. 1, pp. 72–76, 2013.
- [98] I. Repins, C. Beall, N. Vora et al., "Co-evaporated  $\text{Cu}_2\text{ZnSnSe}_4$  films and devices," *Solar Energy Materials & Solar Cells*, vol. 101, pp. 154–159, 2012.
- [99] D. A. R. Barkhouse, R. Haight, N. Sakai, H. Hiroi, H. Sugimoto, and D. B. Mitzi, "Cd-free buffer layer materials on  $\text{Cu}_2\text{ZnSn}(\text{S}_x\text{Se}_{1-x})_4$ : Band alignments with  $\text{ZnO}$ ,  $\text{ZnS}$ , and  $\text{In}_2\text{S}_3$ ," *Applied Physics Letters*, vol. 100, no. 19, p. 193904, 2012.
- [100] T. K. Todorov, J. Tang, S. Bag et al., "Beyond 11% efficiency: Characteristics of state-of-the-art  $\text{Cu}_2\text{ZnSn}(\text{S},\text{Se})_4$  Solar Cells," *Advanced Energy Materials*, vol. 3, no. 1, pp. 34–38, 2013.
- [101] N. Muhunthan, O. P. Singh, S. Singh, and V. N. Singh, "Growth of CZTS thin films by cosputtering of metal targets and sulfurization in  $\text{H}_2\text{S}$ ," *International Journal of Photoenergy*, vol. 2013, Article ID 752012, 7 pages, 2013.
- [102] C. Platzer-Björkman, C. Frisk, J. K. Larsen et al., "Reduced interface recombination in  $\text{Cu}_2\text{ZnSnS}_4$  solar cells with atomic layer deposition  $\text{Zn}_{1-x}\text{Sn}_x\text{O}_y$  buffer layers," *Applied Physics Letters*, vol. 107, no. 24, p. 243904, 2015.
- [103] K. Sun, F. Liu, C. Yan et al., "Influence of sodium incorporation on kesterite  $\text{Cu}_2\text{ZnSnS}_4$  solar cells fabricated on stainless steel substrates," *Solar Energy Materials and Solar Cells*, vol. 157, pp. 565–571, 2016.
- [104] K. B. Messaoud, M. Buffière, G. Brammertz et al., "Synthesis and characterization of (Cd, Zn) S buffer layer for  $\text{Cu}_2\text{ZnSnSe}_4$  solar cells," *Journal of Physics D: Applied Physics*, vol. 50, no. 28, p. 285501, 2017.
- [105] T. Ericson, F. Larsson, T. Törndahl et al., "Zinc-Tin-Oxide Buffer Layer and Low Temperature Post Annealing Resulting

- in a 9.0% Efficient Cd-Free  $\text{Cu}_2\text{ZnSnS}_4$  Solar Cell,” *Solar RRL*, vol. 1, no. 5, p. 1700001, 2017.
- [106] C. W. Hong, S. W. Shin, M. P. Suryawanshi, M. G. Gang, J. Heo, and J. H. Kim, “Chemically deposited CdS buffer/Kesterite  $\text{Cu}_2\text{ZnSnS}_4$  Solar cells: relationship between CdS thickness and device performance,” *ACS Applied Materials & Interfaces*, vol. 9, no. 42, pp. 36733–36744, 2017.
- [107] S. Bag, O. Gunawan, T. Gokmen, Y. Zhu, and D. B. Mitzi, “Hydrazine-Processed Ge-Substituted CZTSe Solar Cells,” *Chemistry of Materials*, vol. 24, no. 23, pp. 4588–4593, 2012.
- [108] C. J. Hages, S. Levencenco, C. K. Miskin et al., “Improved Performance of Ge-Alloyed CZTGeS<sub>2</sub> Thin-Film Solar Cells through Control of Elemental Losses,” *Progress in Photovoltaics: Research and Applications*, vol. 23, no. 3, pp. 376–384, 2015.
- [109] J. Kim, H. Hiroi, T. K. Todorov et al., “High Efficiency  $\text{Cu}_2\text{ZnSn}(\text{S},\text{Se})_4$  Solar Cells by Applying a Double  $\text{In}_2\text{S}_3/\text{CdS}$  Emitter,” *Advanced Materials*, vol. 26, no. 44, pp. 7427–7431, 2014.
- [110] Y. S. Lee, T. Gershon, O. Gunawan et al., “ $\text{Cu}_2\text{ZnSn}(\text{S},\text{Se})_4$  Thin-Film Solar Cells by Thermal Co-Evaporation with 11.6% Efficiency and Improved Minority Carrier Diffusion Length,” *Advanced Energy Materials*, vol. 5, no. 7, 2015.
- [111] A. Nagoya, R. Asahi, and G. Kresse, “First-principles study of  $\text{Cu}_2\text{ZnSnS}_4$  and the related band offsets for photovoltaic applications,” *Journal of Physics. Condensed Matter*, vol. 23, no. 40, p. 404203, 2011.
- [112] L. A. Burton, D. Colombara, R. D. Abellon et al., “Synthesis, Characterization, and Electronic Structure of Single-Crystal  $\text{SnS}$ ,  $\text{Sn}_2\text{S}_3$ , and  $\text{SnS}_2$ ,” *Chemistry of Materials*, vol. 25, no. 24, pp. 4908–4916, 2013.
- [113] Y. Wu, C. Wadia, W. Ma, B. Sadtler, and A. P. Alivisatos, “Synthesis and Photovoltaic Application of Copper(I) Sulfide Nanocrystals,” *Nano Letters*, vol. 8, no. 8, pp. 2551–2555, 2008.
- [114] K. Ito and T. Nakazawa, “Electrical and Optical Properties of Stannite-Type Quaternary Semiconductor Thin Films,” *Japanese Journal of Applied Physics*, vol. 27, Part 1, 11, pp. 2094–2097, 1988.
- [115] J. Li, Y. Zhang, Y. Wang et al., “Formation of  $\text{Cu}_2\text{ZnSnS}_4$  thin Film Solar Cell by CBD-Annealing Route: Comparison of Cu and CuS in Stacked Layers  $\text{SnS}/\text{Cu}(\text{S})/\text{ZnS}$ ,” *Solar Energy*, vol. 129, pp. 1–9, 2016.
- [116] E. Garcia-Llamas, J. M. Merino, R. Gunder et al., “ $\text{Cu}_2\text{ZnSnS}_4$  thin Film Solar Cells Grown by Fast Thermal Evaporation and Thermal Treatment,” *Solar Energy*, vol. 141, pp. 236–241, 2017.
- [117] J. Tao, J. Liu, L. Chen et al., “7.1% Efficient Co-Electroplated  $\text{Cu}_2\text{ZnSnS}_4$  thin Film Solar Cells with Sputtered CdS Buffer Layers,” *Green Chemistry*, vol. 18, no. 2, pp. 550–557, 2016.
- [118] J. Zhong, Z. Xia, M. Luo et al., “Sulfurization induced surface constitution and its correlation to the performance of solution-processed  $\text{Cu}_2\text{ZnSn}(\text{S},\text{Se})_4$  solar cells,” *Scientific Reports*, vol. 4, no. 1, 2015.
- [119] K. J. Yang, J. H. Sim, D. H. Son et al., “Effects of the Compositional Ratio Distribution with Sulfurization Temperatures in the Absorber Layer on the Defect and Surface Electrical Characteristics of  $\text{Cu}_2\text{ZnSnS}_4$  solar Cells,” *Progress in Photovoltaics: Research and Applications*, vol. 23, no. 12, pp. 1771–1784, 2015.
- [120] X. Liu, H. Cui, W. Li et al., “Improving  $\text{Cu}_2\text{ZnSnS}_4$  (CZTS) Solar Cell Performance by an Ultrathin ZnO Intermediate Layer between CZTS Absorber and Mo Back Contact,” *Physica Status Solidi (RRL) - Rapid Research Letters*, vol. 8, no. 12, pp. 966–970, 2014.
- [121] H. Cui, X. Liu, F. Liu, X. Hao, N. Song, and C. Yan, “Boosting  $\text{Cu}_2\text{ZnSnS}_4$  solar Cells Efficiency by a Thin Ag Intermediate Layer between Absorber and Back Contact,” *Applied Physics Letters*, vol. 104, no. 4, p. 041115, 2014.
- [122] K. Biswas, S. Lany, and A. Zunger, “The electronic consequences of multivalent elements in inorganic solar absorbers: Multivalency of Sn in  $\text{Cu}_2\text{ZnSnS}_4$ ,” *Applied Physics Letters*, vol. 96, no. 20, p. 201902, 2010.
- [123] S. Chen, A. Walsh, X. G. Gong, and S. H. Wei, “Classification of Lattice Defects in the Kesterite  $\text{Cu}_2\text{ZnSnS}_4$  and  $\text{Cu}_2\text{ZnSnSe}_4$  earth-Abundant Solar Cell Absorbers,” *Advanced Materials*, vol. 25, no. 11, pp. 1522–1539, 2013.
- [124] L. Kronik, D. Cahen, and H. W. Schock, “Effects of Sodium on Polycrystalline  $\text{Cu}(\text{In},\text{Ga})\text{Se}_2$  and Its Solar Cell Performance,” *Advanced Materials*, vol. 10, no. 1, pp. 31–36, 1998.
- [125] A. Rockett, “The effect of Na in polycrystalline and epitaxial single-crystal  $\text{CuIn}_{1-x}\text{Ga}_x\text{Se}_2$ ,” in *Thin Solid Films*, vol. 480–481, pp. 2–7, 2005.
- [126] J. V. Li, D. Kuciauskas, M. R. Young, and I. L. Repins, “Effects of Sodium Incorporation in co-Evaporated  $\text{Cu}_2\text{ZnSnSe}_4$  thin-film Solar Cells,” *Applied Physics Letters*, vol. 102, no. 16, p. 163905, 2013.
- [127] N. M. Shinde, D. P. Dubal, D. S. Dhawale, C. D. Lokhande, J. H. Kim, and J. H. Moon, “Room Temperature Novel Chemical Synthesis of  $\text{Cu}_2\text{ZnSnS}_4$ (CZTS) Absorbing Layer for Photovoltaic Application,” *Materials Research Bulletin*, vol. 47, no. 2, pp. 302–307, 2012.
- [128] J. He, L. Sun, S. Chen, Y. Chen, P. Yang, and J. Chu, “Composition dependence of structure and optical properties of  $\text{Cu}_2\text{ZnSn}(\text{S},\text{Se})_4$  solid solutions: An experimental study,” *Journal of Alloys and Compounds*, vol. 511, no. 1, pp. 129–132, 2012.
- [129] A. Khare, A. W. Wills, L. M. Ammerman, D. J. Norris, and E. S. Aydil, “Size Control and Quantum Confinement in  $\text{Cu}_2\text{ZnSnS}_4$  nanocrystals,” *Chemical Communications*, vol. 47, no. 42, pp. 11721–11723, 2011.